Dynamics of *Mycobacterium tuberculosis* Ag85B revealed by sensitive ELISA

Joel D. Ernst[a,b#*], Amber Cornelius[b], and Miriam Bolz[b**]

[a]Division of Experimental Medicine, University of California, San Francisco; [b]Division of Infectious Diseases and Immunology, Department of Medicine, New York University School of Medicine

*Present address:

UCSF Division of Experimental Medicine
1001 Potrero Ave., Box 1234
San Francisco, CA 94110

**Present address:

Swiss Tropical Public Health Institute
Socinstr. 57, CH 4002
University of Basel
Petersplatz 1
CH 4003 Basel, Switzerland

Running title: Ag85B secretion and trafficking

Address for correspondence:

Joel Ernst
UCSF Division of Experimental Medicine
1001 Potrero Ave., Box 1234
San Francisco, CA 94110
joel.ernst@ucsf.edu

Word count for the abstract: 233

Word count for the text: 3,812

Abstract

Secretion of specific proteins contributes to pathogenesis and immune responses in tuberculosis and other bacterial infections, yet the kinetics of protein secretion and fate of secreted proteins in vivo are poorly understood. We generated new monoclonal antibodies that recognize the *M. tuberculosis* secreted protein, Ag85B, and used them to establish and characterize a sensitive ELISA to quantitate Ag85B in samples generated in vitro and in vivo. We found that nutritional or culture conditions had little impact on secretion of Ag85B, and that there is considerable variation in Ag85B secretion by distinct strains in the *M. tuberculosis* complex: compared with the commonly-used H37Rv strain (Lineage 4), *M. africanum* (Lineage 6) secretes less, and two strains from Lineage 2 secrete more Ag85B. We also used the ELISA to determine that the rate of secretion of Ag85B is 10- to 100-fold lower than that of proteins secreted by gram-negative and gram-positive bacteria, respectively. ELISA quantitation of Ag85B in lung homogenates of *M. tuberculosis* H37Rv-infected mice revealed that although Ag85B accumulates in the lungs as the bacterial population expands, the amount of Ag85B per bacterium decreases nearly 10,000-fold at later stages of infection, coincident with development of T cell responses and arrest of bacterial population growth. These results indicate that bacterial protein secretion in vivo is dynamic and regulated, and quantitation of secreted bacterial proteins can contribute to understanding pathogenesis and immunity in tuberculosis and other infections.

Importance

Bacterial protein secretion contributes to host-pathogen interactions, yet the process and consequences of bacterial protein secretion during infection are poorly understood. We developed a sensitive ELISA to quantitate a protein (termed Ag85B) secreted by *M. tuberculosis* and used it to find that Ag85B secretion occurs with slower kinetics than for proteins secreted by gram positive and gram negative bacteria, and that accumulation of Ag85B in the lungs is markedly regulated as a function of the bacterial population density. Our results demonstrate that quantitation of bacterial proteins during infection can reveal novel insights into host-pathogen interactions.

Introduction

Mycobacterium tuberculosis employs secretion of specific proteins (estimated to include up to ~25% of the bacterial proteome (1)) to survive, interact with host targets during infection (2, 3), manipulate its intracellular niche (2-7), and induce protective and pathogenic immune responses (8). Among the proteins that are most abundant in *M. tuberculosis* culture supernatants are members of a family of three closely related proteins, the antigen 85 (Ag85) complex consisting of Ag85A, Ag85B, and Ag85C (9). All three of these proteins exhibit enzymatic activity as mycolyl transferases, in which they catalyze transesterification reactions to synthesize trehalose monomycolate (TMM), trehalose dimycolate (TDM), and mycolated arabinogalactan (10, 11). Because of these enzymatic activities and their importance in constructing the mycobacterial envelope, Ag85A, Ag85B, and Ag85C have been considered potential drug targets for treatment of tuberculosis (10).

Due to their ability to induce adaptive CD4 and CD8 T lymphocyte responses in a broad range of vertebrate hosts, Ag85A and Ag85B have been investigated as antigens for tuberculosis vaccines, and are prominent components of at least seven candidate vaccines in various stages of development (http://www.aeras.org). Quantitative assays of mRNA have revealed that the genes encoding Ag85A and Ag85B (*fbpA* and *fbpB*, respectively) are expressed at high levels by bacteria in the lungs early after aerosol infection of mice, but their mRNA expression decreases markedly after the recruitment of antigen-specific effector T cells to the lungs (12-14). Consistent with the results of bacterial RNA quantitation, CD4 T cells specific for Ag85B are activated in the lungs between two and three weeks after infection of mice, but their activation markedly decreases concurrent with decreased bacterial expression of the *fbpB* gene (12, 15).

Despite considerable knowledge of the properties of the *fbpA* and *fbpB* genes and the antigenicity of their products, there is less information on the secretion, in vivo expression, and

82 trafficking of the Ag85A or Ag85B proteins. Because of interest in Ag85B as a vaccine and/or
83 diagnostic antigen, we generated new monoclonal antibodies to Ag85B and used them to
84 establish a highly sensitive and specific ELISA. We then employed the ELISA in studies of
85 secretion and trafficking of the Ag85B protein in vitro and in vivo.
86

Results

Generation and characterization of monoclonal antibodies to Ag85B

Monoclonal antibodies were generated using standard methods (16), from mice immunized with purified recombinant *M. tuberculosis* Ag85B (rAg85B), expressed in *E. coli*. Three monoclonal antibodies (mAbs), termed 710, 711, and 712, were selected for characterization. When examined by direct ELISA using wells coated with purified rAg85A, rAg85B, or rAg85C, and varying concentrations of antibody, all three mAbs recognized Ag85B, and yielded equivalent signals (Figure 1A). The three mAbs also recognized Ag85A in the direct ELISA, although recognition of Ag85A required higher antibody concentrations and reached lower maximum signal intensity than with Ag85B. mAb 710 generated a higher signal intensity, and at lower antibody concentrations compared with mAbs 711 and 712; the latter two mAbs also exhibited detectable binding to Ag85A when used at concentrations ≥ 1 µg/ml (Figure 1B). In contrast, mAbs 711 and 712 did not bind to Ag85C in direct ELISA at any antibody concentration examined, while mAb 710 bound Ag85C at antibody concentrations as low as 0.01 µg/ml (Figure 1C). Testing of the mAbs at a fixed concentration of 1 µg/ml on a dilution series of recombinant protein in direct ELISA, revealed that mAb 710 bound to Ag85A, Ag85B, and Ag85C at lower antigen concentrations than did mAb 711 or 712; mAbs 711 and 712 were indistinguishable in this assay. All three mAbs bound to Ag85B at lower antigen concentrations than required for binding to Ag85A or Ag85C (Figure 1D-E). Together, these results indicate that mAbs 710, 711, and 712 preferentially recognize Ag85B, although each of the mAbs also binds Ag85A and Ab85C when these antigens are present at high concentrations.

Sandwich ELISA for quantitation of Ag85B

When the three mAbs were used in pairwise combinations, using one mAb for capture, and another mAb conjugated to horseradish peroxidase (HRP) for detection of bound antigen, the

highest sensitivity for detection of Ag85B was obtained when mAb 710 was used as the capture antibody (Figure 2A). Although the differences were slight, sensitivity appeared to be greater when mAb 711 rather than mAb 712 was used as the detecting antibody. Compared with Ag85B capture by mAb 710, mAb 711 capture allowed detection of bound Ag85B by mAb 710 but not by mAb 712. When mAb 712 was used for capture, mAb 710 was able to bind Ag85B, but mAb 711 was not. Together, these data indicate that the epitopes recognized by mAbs 711 and 712 overlap or may even be identical, while the epitope recognized by mAb710 is distinct from those of mAbs 711 and 712. Despite detectable binding of all three mAbs to Ag85A in the direct ELISA (Figure 1B), none of the combinations of capture or detecting antibodies yielded a signal when Ag85A was used as the antigen in the sandwich ELISA (Figure 2B). Likewise, despite binding of mAb 710 to Ag85C by direct ELISA, none of the capture or detecting antibody combinations resulted in a detectable signal in the sandwich ELISA when Ag85C was used as the antigen (Figure 2C). Together, these results suggest that the epitope recognized by mAb 710 is at least partially shared by Ag85A, Ag85B, and Ag85C, while the epitope(s) recognized by mAbs 711 and 712 is more specific to Ag85B.

To confirm specificity of the ELISA with the combination of mAbs 710 and 711 using native *M. tuberculosis* proteins, we examined culture filtrates of wild-type H37Rv and of our previously-characterized Ag85B-deficient (*fbpB* null) mutant strain of H37Rv (12). This yielded no detectable signal in the ELISA when culture filtrates of the Ag85B-deficient bacteria were examined, despite the detection of an abundant signal when wild-type culture filtrates were examined (Figure 2D). Since the Ag85B-null bacteria retain the capacity to synthesize and secrete Ag85A and Ag85C (17), these results provide further evidence that the sandwich ELISA with mAbs 710 and 711 is highly specific for Ag85B.

The assay in this form, with mAb 710 as the capture antibody and HRP-coupled mAb 711 as the detection antibody, has been run in our laboratory >30 times to determine Ag85B content

in various samples. Each assay comprised at least one standard curve with rAg85B per ELISA plate, starting at 10 ng/ml or above and including 2-fold dilutions to loss of signal (generally, ≤20 pg/ml). Three representative assay standard curves are shown in Figure 2E. Ag85B in samples was quantitated based on either a dose-response sigmoidal regression curve or a linear regression in the linear proportion of the curve (0 ng/ml – 2.5 ng/ml). With both methods regression curves had R^2 values > 0.99. When necessary, samples were diluted for ELISA to be in linear range of the standard curve and either at least two technical replicates or biological replicates (when available) were run.

Carbon source effects, strain-dependent variation, and kinetics of Ag85B secretion

We used the ELISA to examine whether Ag85B secretion is governed by bacterial growth conditions. When grown in rich broth (Middlebrook 7H9 medium with 10% albumin-dextrose-catalase), a 10-fold difference in Tween 80 concentration (0.5% vs 0.05%) did not affect the amount of Ag85B secreted by *M. tuberculosis* H37Rv in over a 24 h period (Figure 3A). When H37Rv was grown in minimal defined media (Sauton's medium, with 0.05% Tween 80, 0.5% BSA with 0.05% tyloxapol), or 7H9 broth with the addition of 0.2% acetate, dextrose or glycerol as carbon sources, the addition of acetate or glycerol did not alter Ag85B secretion, whereas 0.2% dextrose increased Ag85B secretion approximately 2-fold (Figure 3A). These results indicate that bacterial metabolism as dictated by alternative carbon sources can affect the rate and/or amount of Ag85B secretion, but that the concentration of Tween 80 had little measurable effect.

We previously reported that *M. africanum* expresses lower levels of Ag85B than *M. tuberculosis* H37Rv, as detected by immunoblotting and by the magnitude of in vivo antigen-specific CD4 T cell responses (18). To verify this result and determine whether other strain-dependent variation in Ag85B secretion exists, we used the Ag85B-specific ELISA to assay culture filtrates from phylogenetically distinct bacterial isolates. This confirmed that *M.*

africanum secretes significantly lower quantities of Ag85B compared with *M. tuberculosis* H37Rv (Figure 3B). We also found that two distinct isolates of *M. tuberculosis* from Lineage 2 (includes the Beijing family) secrete significantly higher quantities of Ag85B than H37Rv (Figure 3B). These results indicate substantial variation in secretion of Ag85B, according to the bacterial strain, possibly in a lineage-dependent manner.

To further characterize the properties of Ag85B, we determined the kinetics of its secretion by *M. tuberculosis* H37Rv. Washed mid-log phase bacteria were suspended in fresh 7H9 media at 10^8 CFU/ml, and culture filtrates were harvested at multiple intervals and assayed by ELISA. The rate of accumulation of Ag85B in culture filtrates was linear ($r^2 = 0.93$) during the 24-hour period of sampling, at 1.8 ± 0.2 ng/ml/hr (Figure 3C). Since the mature Ag85B protein has a molecular weight of 34,580, this is equivalent to 52 fmol per 10^8 CFU/hr, or approximately 300 molecules secreted per bacterial cell/hr.

Cell-free Ag85B during infection in vivo and in vitro

Despite their biological activity and roles in pathogenesis and immune responses, little is known of the in vivo fate or distribution of secreted *M. tuberculosis* proteins, especially during infection. Therefore, we examined supernatants of lung homogenates obtained at various intervals after infecting C57BL/6 mice with *M. tuberculosis* H37Rv by aerosol. We found that Ag85B was detectable in lung homogenate supernatants in some, but not all, mice as early as 4-8 days post-infection, followed by a progressive increase between 14 and 21 days post-infection (Figure 4A). Since the samples for assay were taken during the progressive growth phase of the bacteria in the lungs, the quantity of Ag85B detected is a function of the amount secreted by each bacterium and by the number of bacteria, which increases progressively until approximately 21 days post-infection (19). Therefore, we normalized the concentration of Ag85B in lung homogenates by the number of bacteria present in the lungs at each time point sampled. This revealed a progressive decrease in the amount of Ag85B relative to the

bacterial population size, commencing between 8 and 11 days post infection (Figure 4B). This result is consistent with results of Ag85B RNA quantitation on bacterial populations in the lungs of immunocompetent mice (12-14), and with results of studies indicating that activation of Ag85B-specific CD4 T cells in vivo decreases markedly after 2-3 weeks of infection, due to limited availability of antigen (12, 15).

There are several potential sources of free Ag85B in the lungs. First is that some of the bacteria may be extracellular and may secrete Ag85B directly to the intercellular spaces in lung tissues. Second is that, as we have recently reported, Ag85B and other secreted mycobacterial proteins can be exported from infected cells by a vesicular transport pathway (20, 21). A third potential mechanism is release of Ag85B associated with bacterial membrane vesicles (22) and/or exosomes shed by infected cells (23, 24). A fourth possible mechanism is that Ag85B synthesized by intracellular bacteria may be released from dying infected cells. We investigated the latter possibility, using bone marrow-derived dendritic cells infected with *M. tuberculosis* H37Rv. Under conditions of the multiplicities of infection, bacterial strain, and time points used, we observed a range of loss of cell viability as reflected by luminescence assay of ATP in cell lysates, after harvesting conditioned medium for assay of Ag85B by ELISA. This revealed a correlation between loss of cell viability and the quantity of Ag85B in conditioned media ($r^2 = 0.5777$; $p < 0.0001$) (Figure 5), indicating that Ag85B can be released from dead and/or dying infected cells in a form that remains detectable by ELISA. This suggests that death of infected cells can be a source of the Ag85B detected in cell-free homogenates of the lungs of infected mice, as in Figure 4.

Discussion

In this work, we developed three new murine monoclonal antibodies by immunizing mice with recombinant *M. tuberculosis* Ag85B, and used them to develop a sensitive and specific ELISA for quantitation of Ag85B in various biological samples. We found that, compared with the H37Rv strain from the *M. tuberculosis* complex lineage 4, two isolates from lineage 2 secreted greater quantities, while a lineage 6 (*M. africanum*) isolate secreted lesser quantities of Ag85B. Since Ag85B plays a role in synthesis of trehalose dimycolate, and trehalose dimycolate is a potent proinflammatory mediator during *M. tuberculosis* infection (25-28), the results suggest that differences in Ag85B secretion may contribute to strain-dependent differences in the proinflammatory properties of distinct strains and lineages in the *M. tuberculosis* complex (29). Strain variability in secretion may also influence the frequency and magnitude of T cell responses to Ag85B, which may provide an explanation for the finding that fewer human subjects exhibit detectable responses to Ag85B compared with other antigens such as ESAT-6 and/or CFP-10 (30, 31). Likewise, bacterial strain-dependent variation in secretion of Ag85B may influence the protective efficacy of TB subunit vaccines that include Ag85B: even if a vaccine generates immune responses to Ag85B, vaccination may provide little protection against infection with mycobacterial strains that express and secrete lesser quantities of Ag85B. In studies of subunit vaccines that include Ag85B, it may be informative to characterize Ag85B expression and secretion in the isolates of *M. tuberculosis* from subjects that develop breakthrough infections despite apparently-appropriate immune responses to the vaccine antigen.

We also used the ELISA to determine the rate of secretion by *M. tuberculosis* H37Rv in broth culture as approximately 300 molecules of Ag85B per bacterial cell per hour. This is 10 to 100-fold lower than the rate of translocation of *E. coli* proOmpA (4.5 mol/min) (32), or the secretion of Staphylococcal toxic shock toxin (1.1 x 10^4 molecules/CFU/hr) (33). To fully

understand the basis for this difference will require determination of the rates of protein synthesis in *M. tuberculosis* compared with that of other bacteria, and characterization of the factors and mechanisms that determine the rate of protein secretion by distinct secretion systems in bacteria. Given the important roles of secreted protein virulence factors in *M. tuberculosis* and other bacterial pathogens, better understanding of protein secretion may reveal new targets for therapeutic modulation and reduction of disease and pathogen transmission.

A third major finding in these studies is that *M. tuberculosis* Ag85B can be found in homogenized lung tissue supernatants from infected mice. This finding has several potential implications. If data from studies in human subjects provide supportive data, then detecting Ag85B in respiratory secretions may provide a rapid and economical approach to diagnosis of pulmonary tuberculosis and may also be useful in monitoring responses to treatment. Another is that the presence of extracellular Ag85B in lung tissue may make Ag85B available for uptake and processing and presentation by uninfected dendritic cells and macrophages in the lungs. Since we have reported that direct recognition of infected cells is required for optimal CD4 T cell control of intracellular *M. tuberculosis* (34), acquisition and presentation of Ag85B by uninfected cells in the lungs may provide antigen-loaded decoys for Ag85B-specific CD4 T cells that reduce the frequency of recognition of infected cells by those T cells. This is consistent with our recent finding in mouse lungs (35) and the finding in lungs of *M. tuberculosis*-infected rhesus macaques (36) that only a small fraction of the T cells in the lungs are in close contact with *M. tuberculosis*-infected cells. Our associated finding in this work that death of *M. tuberculosis*-infected host cells can be associated with release of Ag85B to the extracellular space indicates that the presence of Ag85B (and other mycobacterial proteins) in extracellular tissue compartments in the lungs may be the consequence of secretion by extracellular bacteria, vesicular transport from infected cells (21), carriage by exosomes (37,

38), and release by dying or dead host cells. Since Ag85B (39, 40), ESAT-6 (41) and other mycobacterial proteins have been reported to act on host cells to modulate inflammation, our findings provide additional evidence for the plausibility that extracellular mycobacterial proteins contribute to the pathogenesis of TB, and may be susceptible to therapeutic modulation.

Materials and Methods

Ethics statement

All animal experiments were done in accordance with procedures approved by the New York University School of Medicine Institutional Animal Care and Use Committee (Laboratory Animal Care Protocol 150502-01), which conformed to the guidelines provided by the Guide for the care and Use of Laboratory Animals of the National Institutes of Health.

Bacterial strains

The stocks of *M. tuberculosis* H37Rv, H37Rv:Δ*fbpB* (Ag85B-null), 4334, and *M. africanum* 1182 used in our laboratory and for these studies have been previously described (19, 42-44). The *M. tuberculosis* HN878 strain was obtained from BEI Resources.

Recombinant Ag85B

RV1886c-ss.pET23b was transformed into *E. coli* BL21(DE3) pLysS (Invitrogen) and induced with 0.8 mM IPTG for 4 h at 37° C. Cultures were lysed with 50 mM Tris pH 7.0, 150 mM NaCl, lysozyme, benzonase, and 1 mM PMSF for 30 minutes at 22°C on an orbital shaker. The lysate was spun 10,000 x g for 30 minutes, sterile filtered, and loaded onto an AKTA FPLC His-Trap column (GE). The column was washed with 50 mM imidazole, and recombinant protein was eluted with 250 mM imidazole. Purity was assessed by SDS-PAGE.

mAb generation and selection

Balb/C mice were immunized with purified recombinant Ag85B (100 µg/mouse x 2 injections followed by 50 µg/mouse for 2 additional injections) subcutaneously in TiterMax Gold (TiterMax, Norcross, GA, USA), followed by 50 µg/mouse given intravenously 3 days before

harvesting and using spleen cells in fusions with P3X63Ag8 myeloma cells. Hybridoma supernatants were screened for recognition of rAg85B-coated wells by ELISA.

Direct ELISA for characterization of individual mAbs

Ag85A (BEI Resources NR-14871), Ag85B (our purified recombinant), or Ag85C (BEI Resources NR-14858) were used to coat wells at 0.5 µg/well in PBS and incubated overnight at 4°C. The plates were washed 3 times with PBS pH 7.4 with 0.05 % Tween 20, and blocked with PBS containing 1.0 % BSA for 1 hour. A starting concentration of 5 µg/ml of mAb 710, 711, or 712 was serially diluted and 200 µl/well incubated at room temperature for 2 hours. Plates were washed 5 times and incubated with goat anti-mouse IgG HRP (MP Biomedicals) for 1 hour at room temperature. Plates were washed 7 times and developed with TMB substrate according to the manufacturer's instructions (BD). The reaction was stopped with 2M sulfuric acid and absorbance read at 450 nm with a Synergy H1 micro plate reader (BioTek).

Mycobacterial culture filtrates

M. tuberculosis strains H37RV, 4334, and HN878, or *M. africanum* strain 1182, were inoculated from a 1 ml frozen stock of approximately $3x10^8$ CFU/ml into 10 ml of Middlebrook 7H9 media supplemented with 0.5 % albumin, 0.2 % dextrose and 0.3 mg/100 ml catalase (in the text, termed 7H9) and grown to late log phase. The cultures were then passaged and grown once to mid log phase. Cultures were then collected and spun at 150 x g. The collected supernatant was then spun at 3,750 x g for 5 minutes and washed with PBS. The pellets were then resuspended in fresh 7H9 media and grown for 24 h. The cultures were pelleted and the media was sterile filtered.

Sandwich ELISA development and optimization

Individual mAbs were used at 2.5 µg/ml in 50 µl 0.05 M carbonate-bicarbonate buffer to coat wells overnight at 4° C. The plates were washed 3 times with PBS (pH 7.4) with 0.5% Tween 20 and blocked with PBS containing 1.0% BSA for 1 hour. Antibodies for detection were

conjugated to HRP according to manufacturer's recommendations (Abcam). Briefly, 1 µl of Modifier was mixed with 10 µl of antibody and then added to a vial of HRP Mix. The vial was incubated overnight at room temperature in the dark. After incubation, 1 µl of Quencher was added and mixed. The conjugated antibodies were diluted to 0.5 µg/ml in PBS with 1% BSA and stored in aliquots at -20 °C until first use. Upon thawing, conjugated antibodies were stored at 4 °C.

For ELISA, samples were added to plates coated with the designated antibody and incubated at room temperature for 2 hours, then plates were washed 5 times. The labeled, detecting antibody was added and the plates were incubated at room temperature for 1 hour. Plates were washed 7 times and developed with substrate according to the manufacturers' instructions (BD). The reaction was stopped with 2M sulfuric acid and absorbance read at 450 nm.

Sandwich ELISA application

The routine sandwich ELISA used the procedures as described above, with mAb 710 as the capture antibody used to coat wells, and HRP-conjugated mAb 711 used to detect bound antigen. Signal generation for the HRP reaction used TMB substrate (Thermo Scientific).

Effects of medium and carbon source

After washing in PBS, bacteria were resuspended in 6 ml of distilled water and split among 6 bottles. 10 ml of media was added to the bottles. The media were Middlebrook 7H9 with 10% ADC and either 0.05% or 0.5% Tween 80; or Sauton's broth with 0.05% Tween 80, 0.5% BSA, and 0.05% tyloxapol, with 0.2% (w/v) acetate, glycerol, or dextrose (adapted from (45)), and bacteria were incubated for 24 h prior to preparation of culture filtrates.

Preparation of lung homogenate supernatants from M. tuberculosis-infected mice

C57BL/6 mice were infected by the aerosol route with ~60 CFU/mouse of *M. tuberculosis* H37Rv; lungs were harvested and single-cell suspensions were prepared as previously

334 described (46). After sampling the cell suspensions for determination of bacterial CFU, an
335 aliquot of each sample was sterile-filtered, and Ag85B concentration determined by ELISA.
336 *Culture, infection, and analysis of bone marrow-derived dendritic cell death and release of*
337 *Ag85B.*
338 Bone marrow-derived dendritic cells (BMDC), generated as previously described (20), were
339 seeded in 96-well tissue culture treated plates (Corning) at $2x10^6$/well and rested for 2 hours,
340 then infected overnight with different multiplicities of infection (1, 2, 4 and 8) with *M.*
341 *tuberculosis* H37Rv, treated with Amikacin (200 μg/ml, 40min) in BMDC medium (RPMI1640
342 supplemented with 10% heat-inactivated FBS, 2 mM L-glutamine, 1 mM sodium pyruvate, 1x
343 β-mercaptoethanol, 10 mM HEPES and 12 ng/ml recombinant mouse GM-CSF), washed three
344 times in PBS and further cultured in fresh BMDC medium. CM was harvested 16, 24, 34 and
345 48 hours later, sterile filtered and Ag85B in CM quantified by sandwich ELISA. At each harvest
346 time point infected BMDC were assayed for cell death by CellTiter-Glo (Promega) according to
347 the manufacturer's instructions and signal read as Luminescence with a Synergy H1 micro
348 plate reader (BioTek). For each harvest time point signal from uninfected cells was considered
349 as 100 % viability for determination of loss of viability of infected cells.
350 *Statistical analyses*
351 All statistical analyses were performed using Prism 7 (Graphpad). The specific tests used for
352 data analysis are specified in the individual figure legends.
353 **Funding Information**
354 Supported by funds from the National Institutes of Health (R01 AI051242 and R01 AI124471;
355 J.D.E.) and the Swiss National Science Foundation (P2BSP3-165349; M.B.).
356 **Acknowledgements**
357 We thank Smita Srivastava, Ph.D., for her contributions to the initial stages of this project.
358

References

1. Miller BK, Zulauf KE, Braunstein M. 2017. The Sec Pathways and Exportomes of Mycobacterium tuberculosis. Microbiol Spectr 5.

2. Mehra A, Zahra A, Thompson V, Sirisaengtaksin N, Wells A, Porto M, Koster S, Penberthy K, Kubota Y, Dricot A, Rogan D, Vidal M, Hill DE, Bean AJ, Philips JA. 2013. Mycobacterium tuberculosis type VII secreted effector EsxH targets host ESCRT to impair trafficking. PLoS Pathog 9:e1003734.

3. Penn BH, Netter Z, Johnson JR, Von Dollen J, Jang GM, Johnson T, Ohol YM, Maher C, Bell SL, Geiger K, Golovkine G, Du X, Choi A, Parry T, Mohapatra BC, Storck MD, Band H, Chen C, Jager S, Shales M, Portnoy DA, Hernandez R, Coscoy L, Cox JS, Krogan NJ. 2018. An Mtb-Human Protein-Protein Interaction Map Identifies a Switch between Host Antiviral and Antibacterial Responses. Mol Cell 71:637-648.e5.

4. Manzanillo PS, Shiloh MU, Portnoy DA, Cox JS. 2012. Mycobacterium tuberculosis activates the DNA-dependent cytosolic surveillance pathway within macrophages. Cell Host Microbe 11:469-80.

5. Simeone R, Bobard A, Lippmann J, Bitter W, Majlessi L, Brosch R, Enninga J. 2012. Phagosomal rupture by Mycobacterium tuberculosis results in toxicity and host cell death. PLoS Pathog 8:e1002507.

6. Simeone R, Sayes F, Song O, Groschel MI, Brodin P, Brosch R, Majlessi L. 2015. Cytosolic access of Mycobacterium tuberculosis: critical impact of phagosomal acidification control and demonstration of occurrence in vivo. PLoS Pathog 11:e1004650.

7. van der Wel N, Hava D, Houben D, Fluitsma D, van Zon M, Pierson J, Brenner M, Peters PJ. 2007. M. tuberculosis and M. leprae translocate from the phagolysosome to the cytosol in myeloid cells. Cell 129:1287-98.

383 8. Woodworth JS, Cohen SB, Moguche AO, Plumlee CR, Agger EM, Urdahl KB, Andersen
384 P. 2017. Subunit vaccine H56/CAF01 induces a population of circulating CD4 T cells that
385 traffic into the Mycobacterium tuberculosis-infected lung. Mucosal Immunol 10:555-564.
386 9. Wiker HG, Harboe M. 1992. The antigen 85 complex: a major secretion product of
387 Mycobacterium tuberculosis. Microbiological Reviews 56:648-661.
388 10. Backus KM, Dolan MA, Barry CS, Joe M, McPhie P, Boshoff HI, Lowary TL, Davis BG,
389 Barry CE, 3rd. 2014. The three Mycobacterium tuberculosis antigen 85 isoforms have unique
390 substrates and activities determined by non-active site regions. J Biol Chem 289:25041-53.
391 11. Belisle JT, Vissa VD, Sievert T, Takayama K, Brennan PJ, Besra GS. 1997. Role of the
392 major antigen of Mycobacterium tuberculosis in cell wall biogenesis. Science 276:1420-2.
393 12. Bold TD, Banaei N, Wolf AJ, Ernst JD. 2011. Suboptimal activation of antigen-specific
394 CD4+ effector cells enables persistence of M. tuberculosis in vivo. PLoS Pathog 7:e1002063.
395 13. Rogerson BJ, Jung YJ, LaCourse R, Ryan L, Enright N, North RJ. 2006. Expression
396 levels of Mycobacterium tuberculosis antigen-encoding genes versus production levels of
397 antigen-specific T cells during stationary level lung infection in mice. Immunology 118:195-201.
398 14. Shi L, North R, Gennaro ML. 2004. Effect of growth state on transcription levels of
399 genes encoding major secreted antigens of Mycobacterium tuberculosis in the mouse lung.
400 Infect Immun 72:2420-4.
401 15. Moguche AO, Musvosvi M, Penn-Nicholson A, Plumlee CR, Mearns H, Geldenhuys H,
402 Smit E, Abrahams D, Rozot V, Dintwe O, Hoff ST, Kromann I, Ruhwald M, Bang P, Larson RP,
403 Shafiani S, Ma S, Sherman DR, Sette A, Lindestam Arlehamn CS, McKinney DM, Maecker H,
404 Hanekom WA, Hatherill M, Andersen P, Scriba TJ, Urdahl KB. 2017. Antigen Availability
405 Shapes T Cell Differentiation and Function during Tuberculosis. Cell Host Microbe 21:695-
406 706.e5.

16. Greenfield EA (ed). 2014. Antibodies: a laboratory manual. Cold Spring Harbor Laboratory Press, Cold Spring Harbor, New York.

17. Grace PS, Ernst JD. 2016. Suboptimal Antigen Presentation Contributes to Virulence of Mycobacterium tuberculosis In Vivo. J Immunol 196:357-64.

18. Bold TD, Davis DC, Penberthy KK, Cox LM, Ernst JD, de Jong BC. 2012. Impaired fitness of Mycobacterium africanum despite secretion of ESAT-6. J Infect Dis 205:984-90.

19. Wolf AJ, Desvignes L, Linas B, Banaiee N, Tamura T, Takatsu K, Ernst JD. 2008. Initiation of the adaptive immune response to Mycobacterium tuberculosis depends on antigen production in the local lymph node, not the lungs. J Exp Med 205:105-15.

20. Srivastava S, Ernst JD. 2014. Cell-to-cell transfer of M. tuberculosis antigens optimizes CD4 T cell priming. Cell Host Microbe 15:741-52.

21. Srivastava S, Grace PS, Ernst JD. 2016. Antigen Export Reduces Antigen Presentation and Limits T Cell Control of M. tuberculosis. Cell Host Microbe 19:44-54.

22. Lee J, Kim SH, Choi DS, Lee JS, Kim DK, Go G, Park SM, Kim SH, Shin JH, Chang CL, Gho YS. 2015. Proteomic analysis of extracellular vesicles derived from Mycobacterium tuberculosis. Proteomics 15:3331-7.

23. Giri PK, Kruh NA, Dobos KM, Schorey JS. 2010. Proteomic analysis identifies highly antigenic proteins in exosomes from M. tuberculosis-infected and culture filtrate protein-treated macrophages. Proteomics 10:3190-202.

24. Ramachandra L, Qu Y, Wang Y, Lewis CJ, Cobb BA, Takatsu K, Boom WH, Dubyak GR, Harding CV. 2010. Mycobacterium tuberculosis synergizes with ATP to induce release of microvesicles and exosomes containing major histocompatibility complex class II molecules capable of antigen presentation. Infect Immun 78:5116-25.

25. Ishikawa E, Ishikawa T, Morita YS, Toyonaga K, Yamada H, Takeuchi O, Kinoshita T, Akira S, Yoshikai Y, Yamasaki S. 2009. Direct recognition of the mycobacterial glycolipid, trehalose dimycolate, by C-type lectin Mincle. J Exp Med 206:2879-88.

26. Miyake Y, Toyonaga K, Mori D, Kakuta S, Hoshino Y, Oyamada A, Yamada H, Ono K, Suyama M, Iwakura Y, Yoshikai Y, Yamasaki S. 2013. C-type lectin MCL is an FcRgamma-coupled receptor that mediates the adjuvanticity of mycobacterial cord factor. Immunity 38:1050-62.

27. Schoenen H, Bodendorfer B, Hitchens K, Manzanero S, Werninghaus K, Nimmerjahn F, Agger EM, Stenger S, Andersen P, Ruland J, Brown GD, Wells C, Lang R. 2010. Cutting edge: Mincle is essential for recognition and adjuvanticity of the mycobacterial cord factor and its synthetic analog trehalose-dibehenate. J Immunol 184:2756-60.

28. Shenderov K, Barber DL, Mayer-Barber KD, Gurcha SS, Jankovic D, Feng CG, Oland S, Hieny S, Caspar P, Yamasaki S, Lin X, Ting JP, Trinchieri G, Besra GS, Cerundolo V, Sher A. 2013. Cord factor and peptidoglycan recapitulate the Th17-promoting adjuvant activity of mycobacteria through mincle/CARD9 signaling and the inflammasome. J Immunol 190:5722-30.

29. Portevin D, Gagneux S, Comas I, Young D. 2011. Human macrophage responses to clinical isolates from the Mycobacterium tuberculosis complex discriminate between ancient and modern lineages. PLoS Pathog 7:e1001307.

30. Cardoso FLL, Antas PRZ, Milagres AS, Geluk A, Franken KLMC, Oliveira EB, Teixeira HC, Nogueira SA, Sarno EN, Klatser P, Ottenhoff THM, Sampaio EP. 2002. T-Cell Responses to the Mycobacterium tuberculosis-Specific Antigen ESAT-6 in Brazilian Tuberculosis Patients. Infection and Immunity 70:6707-6714.

453 31. Mustafa AS, Amoudy HA, Wiker HG, Abal AT, Ravn P, Oftung F, Andersen P. 1998.
454 Comparison of antigen-specific T-cell responses of tuberculosis patients using complex or
455 single antigens of Mycobacterium tuberculosis. Scand J Immunol 48:535-43.
456 32. De Keyzer J, Van Der Does C, Driessen AJ. 2002. Kinetic analysis of the translocation
457 of fluorescent precursor proteins into Escherichia coli membrane vesicles. J Biol Chem
458 277:46059-65.
459 33. Yarwood JM, Schlievert PM. 2000. Oxygen and carbon dioxide regulation of toxic shock
460 syndrome toxin 1 production by Staphylococcus aureus MN8. J Clin Microbiol 38:1797-803.
461 34. Srivastava S, Ernst JD. 2013. Cutting edge: Direct recognition of infected cells by CD4
462 T cells is required for control of intracellular Mycobacterium tuberculosis in vivo. J Immunol
463 191:1016-20.
464 35. Ernst JD, Cornelius A, Desvignes L, Tavs J, Norris BA. 2018. Limited Antimycobacterial
465 Efficacy of Epitope Peptide Administration Despite Enhanced Antigen-Specific CD4 T-Cell
466 Activation. J Infect Dis 218:1653-1662.
467 36. Kauffman KD, Sallin MA, Sakai S, Kamenyeva O, Kabat J, Weiner D, Sutphin M,
468 Schimel D, Via L, Barry CE, 3rd, Wilder-Kofie T, Moore I, Moore R, Barber DL. 2018. Defective
469 positioning in granulomas but not lung-homing limits CD4 T-cell interactions with
470 Mycobacterium tuberculosis-infected macrophages in rhesus macaques. Mucosal Immunol
471 11:462-473.
472 37. Kruh-Garcia NA, Wolfe LM, Chaisson LH, Worodria WO, Nahid P, Schorey JS, Davis
473 JL, Dobos KM. 2014. Detection of Mycobacterium tuberculosis peptides in the exosomes of
474 patients with active and latent M. tuberculosis infection using MRM-MS. PLoS One 9:e103811.
475 38. Smith VL, Cheng Y, Bryant BR, Schorey JS. 2017. Exosomes function in antigen
476 presentation during an in vivo Mycobacterium tuberculosis infection. Sci Rep 7:43578.

39. Kuo CJ, Ptak CP, Hsieh CL, Akey BL, Chang YF. 2013. Elastin, a novel extracellular matrix protein adhering to mycobacterial antigen 85 complex. J Biol Chem 288:3886-96.

40. Tsujimura Y, Inada H, Yoneda M, Fujita T, Matsuo K, Yasutomi Y. 2014. Effects of mycobacteria major secretion protein, Ag85B, on allergic inflammation in the lung. PLoS One 9:e106807.

41. Volkman HE, Pozos TC, Zheng J, Davis JM, Rawls JF, Ramakrishnan L. 2010. Tuberculous granuloma induction via interaction of a bacterial secreted protein with host epithelium. Science 327:466-9.

42. Copin R, Wang X, Louie E, Escuyer V, Coscolla M, Gagneux S, Palmer GH, Ernst JD. 2016. Within Host Evolution Selects for a Dominant Genotype of Mycobacterium tuberculosis while T Cells Increase Pathogen Genetic Diversity. PLoS Pathog 12:e1006111.

43. Wiens KE, Ernst JD. 2016. The Mechanism for Type I Interferon Induction by Mycobacterium tuberculosis is Bacterial Strain-Dependent. PLoS Pathog 12:e1005809.

44. Wiens KE, Ernst JD. 2016. Type I Interferon is Pathogenic During Chronic Mycobacterium africanum Infection. J Infect Dis 214:1893-1896.

45. de Carvalho LP, Fischer SM, Marrero J, Nathan C, Ehrt S, Rhee KY. 2010. Metabolomics of Mycobacterium tuberculosis reveals compartmentalized co-catabolism of carbon substrates. Chem Biol 17:1122-31.

46. Wolf AJ, Linas B, Trevejo-Nunez GJ, Kincaid E, Tamura T, Takatsu K, Ernst JD. 2007. Mycobacterium tuberculosis infects dendritic cells with high frequency and impairs their function in vivo. J Immunol 179:2509-19.

Figure Legends

Figure 1. Recognition of Ag85A, Ag85B, and Ag85C by monoclonal antibodies 710, 711, and 712. Panels A-C: Wells of 96-well plates were coated with Ag85B (panel A), Ag85A (panel B), or Ag85C (panel C), each at 0.5 µg/ml. Monoclonal Abs 710, 711, or 712 were added at the indicated concentrations, and binding was detected after washing, using horseradish peroxidase (HRP)-conjugated goat anti-mouse IgG and TMB substrate. Data shown in Panels A-C are representative of three independent experiments with one technical replicate per experiment per condition. **Panels D-F:** Individual wells were coated with a dilution series of Ag85B (panel D), Ag85A (panel E), or Ag85C (panel F), starting at 20 µg/ml. Monoclonal Abs 710, 711, or 712 were added at a concentration of 1 µg/ml, and binding was detected after washing, using horseradish peroxidase (HRP)-conjugated goat anti-mouse IgG and TMB substrate. Data in panels D-F are representative of two independent experiments with one technical replicate per experiment per condition.

Figure 2. Characterization of sandwich ELISA for Ag85B. Each mAb was tested as the capture antibody, with either of the remaining two mAbs (conjugated to HRP) used for detection. A) Detection of rAg85B added to mAb-coated plates at the concentrations indicated on the X axis. B) Detection of rAg85A under the same conditions as in panel A. The inset shows the same data on a contracted scale, to reveal small differences. C) Detection of rAg85C under the same conditions as in panel A. The inset shows the same data on a contracted scale, to reveal small differences. D) Specificity of ELISA using mAb 710 for capture and HRP-conjugated mAb 711 for detection of antigen in culture filtrates of wild-type *M. tuberculosis* H37Rv or *M. tuberculosis* H37Rv with a targeted deletion of the gene encoding Ag85B. The H37Rv culture filtrate was diluted to give a signal in the linear range of the ELISA standard curve, while the H37RvΔAg85B culture filtrate was assayed undiluted. The date shown are mean (bar) and standard deviation (error bar) of biological triplicate values. E)

525 Standard curves of rAg85B in Ag85B ELISA. Shown are curves of three independent
526 experiments with two independent standard curves each. Shown are mean (dot) and standard
527 deviation (error bar) when large enough to depict.
528 Data shown in Panels A-C are representative of three independent experiments with one
529 technical replicate per experiment per condition.
530 **Figure 3. Effects of carbon source and *M. tuberculosis* strain, and kinetics of Ag85B**
531 **secretion.** A) Effects of media composition and carbon source on Ag85B secretion. Mid-log
532 phase bacteria (A_{600} = 1.0) grown in 7H9 medium were washed 5 times, then diluted 10-fold
533 into the indicated media. After 24 h, the A_{600} was determined for each culture, and sterile
534 filtrates were prepared for analysis by mAb 710-711 ELISA. Results of Ag85B quantitation by
535 ELISA were normalized by the A_{600} of the individual culture. 7H9 0.05% T80: Middlebrook 7H9
536 with 10% ADC and 0.05% (v/v) Tween 80; 7H9 0.5% T80: same as preceding, but with 0.5%
537 Tween 80; Sau: Sauton's medium with 0.05% Tween 80; Ace: 7H9 media with acetate; Dex:
538 7H9 media with dextrose; Gly: 7H9 media with glycerol. Show are mean (bar) and standard
539 deviation (error bar) of biological triplicate values. Statistical comparison was done using one-
540 way ANOVA; the adjusted p value after Dunnett's post-test for multiple comparisons was
541 applied is shown for the effect of dextrose. Other effects were not significant after adjusting for
542 multiple comparisons. B) Mycobacterial strain-dependent variation of Ag85B secretion. Mid-log
543 phase cultures were collected and the bacteria from each strain were washed and
544 resuspended in fresh 7H9 broth. After 24h, the bacteria were pelleted by centrifugation and
545 Ag85B in culture filtrates was quantitated by ELISA. Show are mean (bar) and standard
546 deviation (error bar) of biological triplicate values. The adjusted p values shown are for
547 comparison of each strain with H37Rv, and were determined by one-way ANOVA with
548 Dunnett's post-test. C) Kinetics of Ag85B secretion by *M. tuberculosis* H37Rv. Mid-log phase
549 growing H37Rv was washed, added to fresh 7H9 medium at 1 x 10^8 CFU/ml, and incubated for

24 h. Individual cultures were sampled at the designated time points and culture filtrates were assayed by ELISA. Statistical analysis by linear regression was determined using Prism 7. Dashed lines indicate 95% confidence interval. Figure A shows one representative of three independent experiments. Figures B and C show data of experiments each done once.

Figure 4. Quantitation of Ag85B in supernatants of lung homogenates from mice infected with *M. tuberculosis* H37Rv. A) *M. tuberculosis* colony-forming units (CFU) in the lung samples used for assays in panel B. B) Ag85B concentrations quantitated by ELISA in lung homogenate supernatants; C) Ag85B concentrations as in Panel B, normalized by the number of bacteria (CFU) in the same lung homogenates. Shown are individual data points, mean ± standard deviation. This experiment was done once.

Figure 5. Death of *M. tuberculosis*-infected primary dendritic cells releases Ag85B. Bone marrow-derived dendritic cells were infected with *M. tuberculosis* H37Rv at different multiplicities of infection (1, 2, 4 and 8). At designated time points (12 h grey dots, 16 h medium blue dots, 24 h red dots, 36 h light blue dots, 48h dark blue dots), medium was removed for quantitation by ELISA, and dendritic cell viability was assessed by luminescence assay of ATP of cell lysates. Results of the two assays on a given sample were plotted as a data point, and Pearson correlation was determined for the whole dataset. Shown are representative results of two similar experiments.

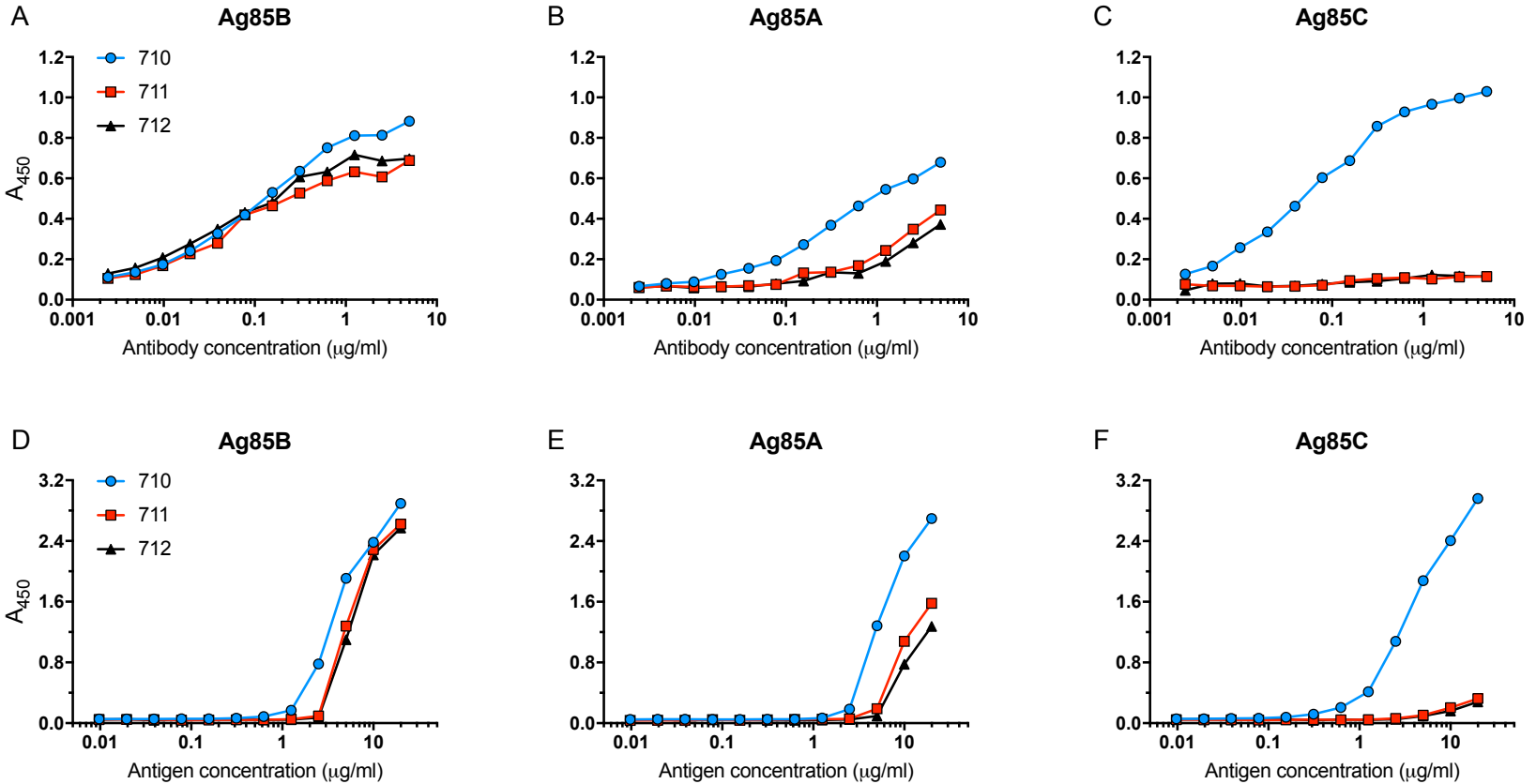
A
Ag85B
710
711
712
A_{450}
1.2
1.0
0.8
0.6
0.4
0.2
0.0
0.001
0.01
0.1
1
10
Antibody concentration (μg/ml)
B
Ag85A
Antibody concentration (μg/ml)
C
Ag85C
Antibody concentration (μg/ml)
D
Ag85B
3.2
2.4
1.6
0.8
0.0
0.01
0.1
1
10
Antigen concentration (μg/ml)
E
Ag85A
Antigen concentration (μg/ml)
F
Ag85C
Antigen concentration (μg/ml)

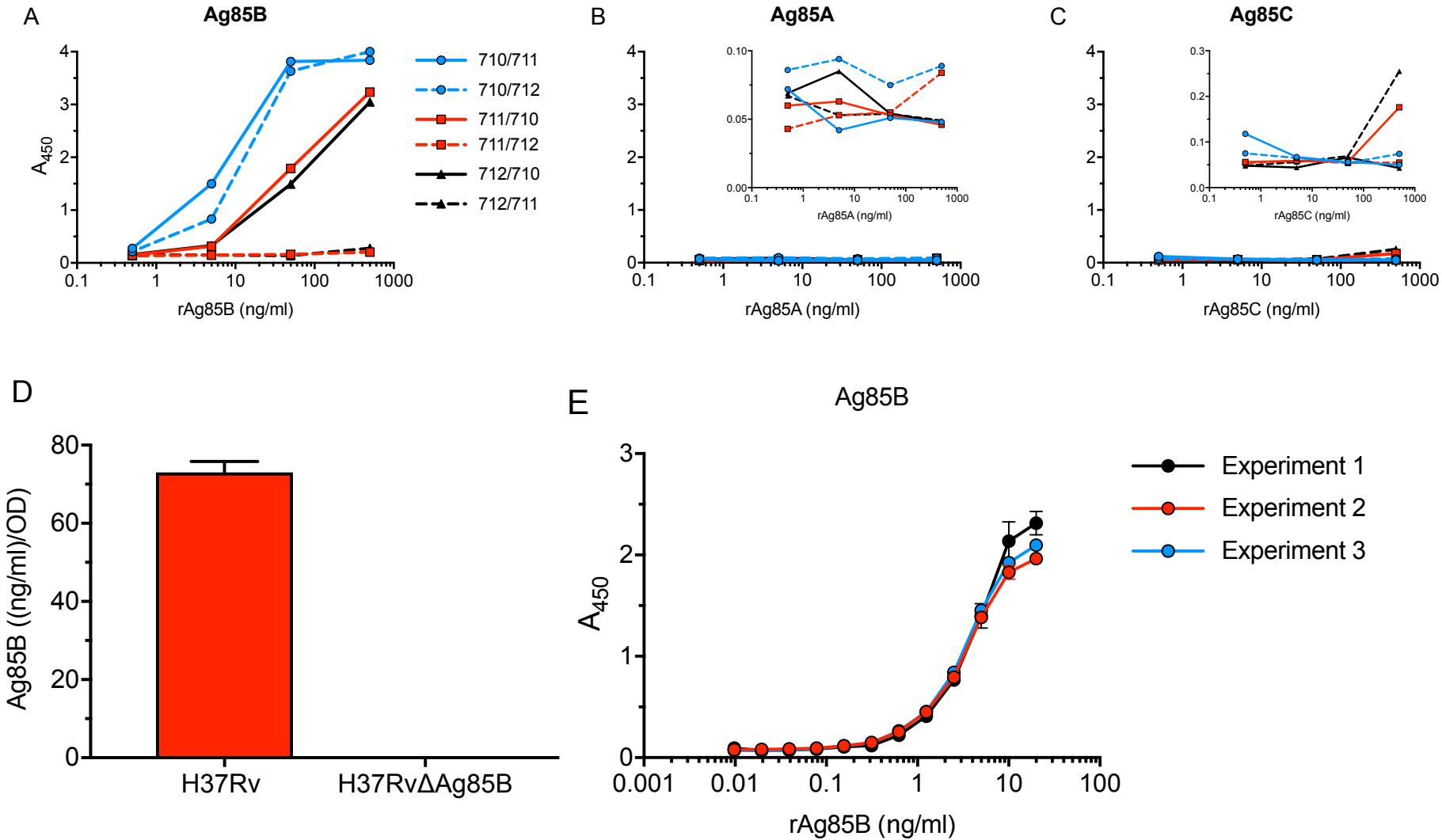
A
Ag85B
710/711
710/712
711/710
711/712
712/710
712/711
A450
rAg85B (ng/ml)
B
Ag85A
rAg85A (ng/ml)
C
Ag85C
rAg85C (ng/ml)
D
Ag85B ((ng/ml)/OD)
H37Rv
H37RvΔAg85B
E
Ag85B
Experiment 1
Experiment 2
Experiment 3
A450
rAg85B (ng/ml)

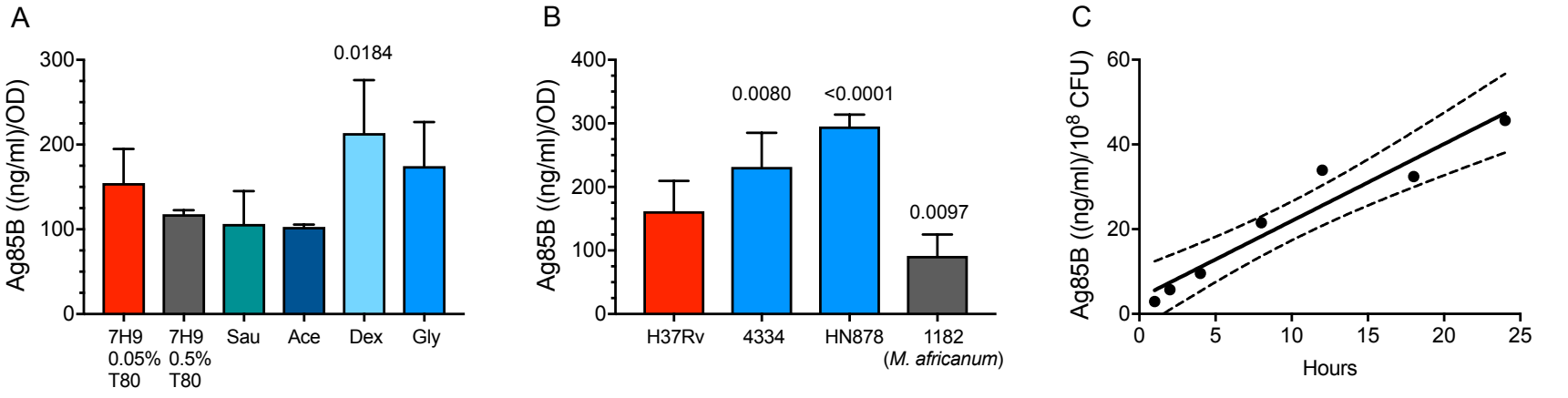
A
Ag85B ((ng/ml)/OD)
300
200
100
0
0.0184
7H9 0.05% T80
7H9 0.5% T80
Sau
Ace
Dex
Gly
B
Ag85B ((ng/ml)/OD)
400
300
200
100
0
0.0080
<0.0001
0.0097
H37Rv
4334
HN878
1182
(M. africanum)
C
Ag85B ((ng/ml)/10^8 CFU)
60
40
20
0
0
5
10
15
20
25
Hours

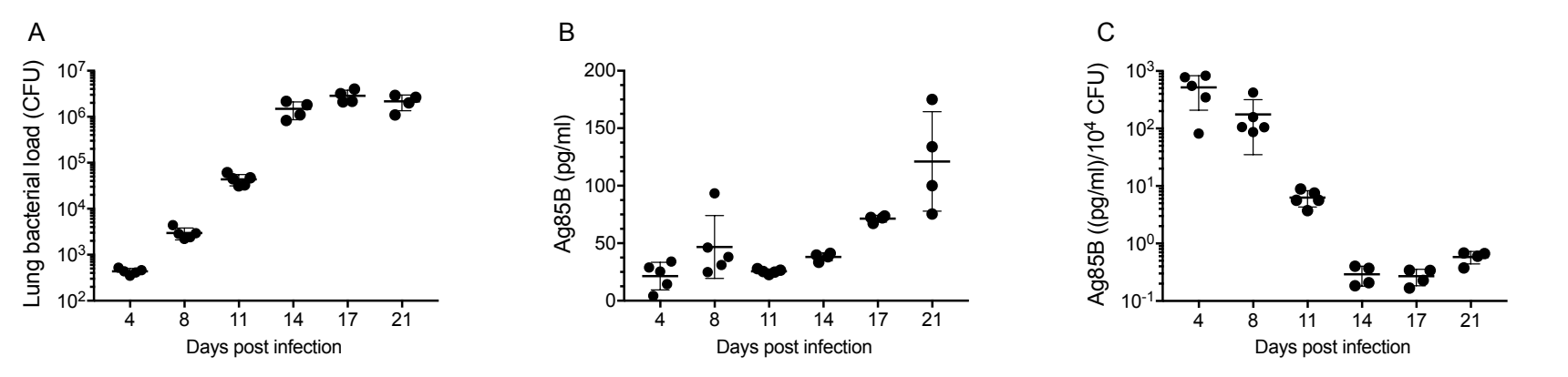
A
Lung bacterial load (CFU)
10^7
10^6
10^5
10^4
10^3
10^2
4
8
11
14
17
21
Days post infection
B
Ag85B (pg/ml)
200
150
100
50
0
4
8
11
14
17
21
Days post infection
C
Ag85B ((pg/ml)/10^4 CFU)
10^3
10^2
10^1
10^0
10^{-1}
4
8
11
14
17
21
Days post infection

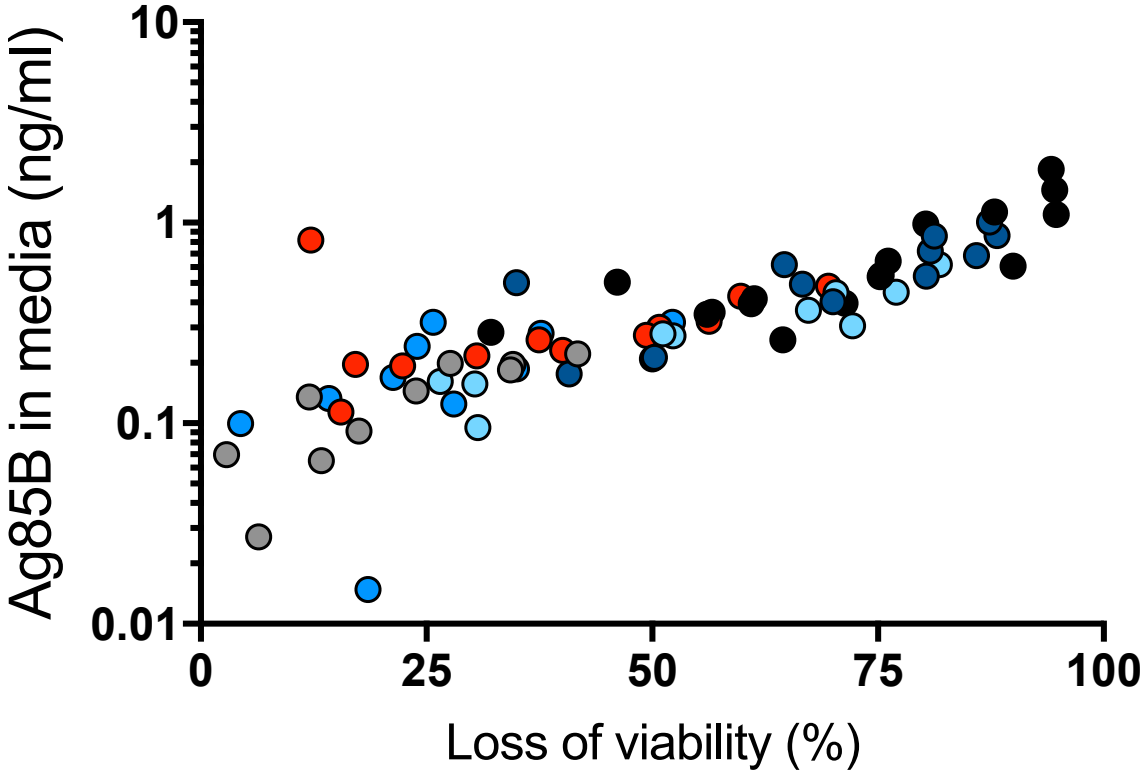
Ag85B in media (ng/ml)
10
1
0.1
0.01
0
25
50
75
100
Loss of viability (%)